Penerbit Akademia Baru

Journal of Advanced Research in Fluid Mechanics and Thermal Sciences

Journal homepage: www.akademiabaru.com/arfmts.html
ISSN: 2289-7879

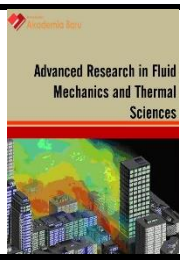

Surface Roughness Effect on Vortex-Induced Vibration Phenomenon in Cross-Flow Direction of a Bluff Body

Open Access

Mohd Kushairi Mohd Ghazali[1], Nik Mohd Ridzuan Shaharuddin[1,*], Arifah Ali[1], Kang Hooi Siang[2], Mohd Nazri Mohd Nasir[1], Mat Hussin Ab. Talib[1]

[1] School of Mechanical Engineering, Faculty of Engineering, Universiti Teknologi Malaysia, 81310 Skudai, Johor, Malaysia
[2] Marine Technology Center, Universiti Teknologi Malaysia, 81310 Skudai, Johor, Malaysia

ARTICLE INFO

Article history:
Received 22 August 2019
Received in revised form 27 September 2019
Accepted 7 October 2019
Available online 28 December 2019

ABSTRACT

This paper presents the experimental result concerning the effect of surface roughness towards the vortex-induced vibration phenomenon on the offshore structure such as riser, which is represented by a bluff body. VIV can cause fatigue damage which is due to excessive vibration in the long run. Simultaneously, the unwanted aquatic organism will be developed at a certain depth of the underwater structure and the roughness of the structure will be changed dramatically. Therefore, it is crucial to investigate the effect of the surface roughness towards the VIV. In this study, A modelled cylinder pipe was mounted on a linear slider with two springs attached at both of its ends in a working section of a circulating water tank. Sandpaper with roughness coefficient varied from 0.19×10^{-3} to 5.10×10^{-3} was utilized to represent different surface roughness on the modelled body. The test covered the subcritical range of Reynolds number from 4.9×10^{3} to 1.5×10^{4}. The displacement of the body was measured at different reduced speeds. The results show that as the surface roughness of the body increases, the amplitude response decreases.

Keywords:
Marine growth; Roughness coefficient; Surface roughness; vortex induced vibration

1. Introduction

As its name implies, vortex-induced vibration (VIV) is a natural phenomenon that normally occurred to a bluff body either in air or water when exposed to the free-flowing stream in a single direction. Marine riser is one of the examples of the fluid-structure interaction phenomenon where the structure vibrates significantly in transverse direction with respect to the stream direction. The vibration will become excessive when the frequency of the vortices shed behind the bluff body is close enough to the structure frequency. This condition is often called as synchronization or lock-in [1]. If the lock-in happens continuously for an extended period, the structure might subject to catastrophic failure due to fatigue damage. However, in real situation over a certain period, the marine structure surface will change due to marine growth and affect the vibration level of vortex-

* *Corresponding author.*
E-mail address: ridzuan@mail.fkm.utm.my/nmridzuan@utm.my (Nik Mohd Ridzuan Shaharuddin)

induced vibration. The occurrence of marine growth starts with the formation of slime, comprising bacteria and diatoms. These are then transformed to algae and in turn on to animal foulers such as barnacles and the process continues until the fully developed community. The marine bacteria immediately dominate on non-toxic surface, with the growth rate of several hundred in a few minutes, several thousand within a few hours and several million within two to three days [2]. This process is often called colonization. Marine organism comprises of various vegetal and animal species based on their location along with the depth of the marine structure with respect of the seawater level [3].

Schoefs [3] classified the marine growth into i) rigid marine growth such as mussels, barnacles, and tubeworms comprising rigid external skeleton-like calcareous shell, ii) soft marine growth such as kelps, soft corals, anemones, hydroids, and iii) whose body texture varies like long kelps. The species were also categorized according to preference area of colonization; area near to surface, medium area and deep area which produces different loading and drag acting on the horizontal and vertical components. The various classification affects the modelling of marine growth as it brings to many uncertainty factors. For example, there are uncertainties in thickness estimation, force measurement in laboratory, and evaluation of loadings. This consequently causes the difficulties in modelling marine growth using numerical and experimental methods, as discussed by Zeinoddini *et al.,* [4]. Research on the marine growth fouling should consider the significant uncertainty source in term of diameter increment and hydrodynamic coefficients level [3].

However, the focus should be given to the type of rigid marine growth as the organism always quickly grow on the surface of the structure that place in underwater. Practically, the surface roughness of the structure will increase because marine organism flourishes on the offshore structure from time to time. The roughness on the surface of the structure will quickly change and consequently modify the flow around the structure. From that, it would increase the induced force produced by wave and the current around the structure [4]. The marine organism will also change the hydrodynamic behaviour [5]. The changes due to marine growth lead to over-loading effect due to screen and drag effects, bio-chemical attacks of materials and mask effects for inspections methods [3]. Besides that, marine fouling can cause additional mass to the structure, and this would decrease the natural frequencies of the structure. When the natural frequency decreases, the chance of frequency synchronization is much higher, and this would lead to large amplitude vibration [6].

There are several factors that can affect the VIV which are the waves induced heave motion of platform, high natural period, surface current and surface of the riser. Hence, the effect of growth of marine organism on the surface roughness is essential to the VIV phenomenon of offshore structures. There are several studies conducted by previous researchers to analyze the effect of thickness of the surface roughness towards VIV. For instance, Kiu *et al.,* [7] investigated the roughness of towed vertical cylinder at subcritical Reynolds numbers of $1.7 \times 10^4 < Re < 8.3 \times 10^4$ and concluded the higher surface roughness result to decrease of maximum transverse response amplitudes, maximum mean drag coefficient and width of the lock-in region. However, it was found that the Strouhal number increased as the surface roughness increased. The reduction of mean drag coefficient of cylinder was also shown in work of Zhou *et al.,* [8] at particular large Reynolds numbers. It was also found that the lift coefficient for rough cylinder is smaller compared to smooth cylinder. The mentioned reductions show the roughness effect favourably reduce the VIV.

However, it should be noted that the effect of roughness depends on the experiment conditions especially the Reynold number, as the roughness can be the enhancement or suppression factor of VIV [4,9]. Result in Bernitsas *et al.,* [9] shows cylinder with roughness strip have higher frequency ratio and amplitude ratio (A/D) as compared to smooth cylinder. The range of Reynold Number used is $8 \times 10^3 < Re < 2.0 \times 10^5$. The result of the work stated that the rough surface could suppress VIV

but with specific experimental condition and model design. Zhou *et al.,* [8] also highlighted the change of effect of surface roughness on VIV response of cylinder; which is favourable at subcritical Reynolds number range and becomes unfavourable at critical range. The effectiveness of suppression for circular cylinder due to marine growth can be found in Skaugset and Baarholm [5]. Artificial hard and soft marine growth were prepared in the study with the Reynolds number ranges from about 1.5 × 10^4 to 9.0 × 10^4. The result presented the marine growth reduce the effectiveness of helical strake with the larger response from soft marine growth.

Experimental studies on the surface roughness effect towards the VIV phenomenon have been conducted using different surface roughness properties of the simulated marine growth. As reported by Kiu *et al.,* [7], the marine growth was simulated following the early method by Achenbach in 1971, who used the emery paper and glued it on the surface of the cylinder. Glueing emery or sandpaper on the surface becomes the most common method in simulating the roughness [7]. The previous research, as summarized in Table 1, used sandpaper, strips, gravel, dimple and pyramidal pattern to imitate the roughness texture. Different roughness coefficient, *k*/*D* and roughness texture were chosen to simulate the surface roughness. The range of roughness coefficient is recorded as it may affect the result of the VIV response.

Table 1
Previous investigations related with surface roughness on VIV for bluff body

Authors	Kiu [7]	Chang *et al.,* [10]	Park *et al.,* [11]	Bernitsas *et al.,* [9]	Gao *et al.,* [6]	Zhou *et al.,* [12]	Zeinoddini *et al.,* [4]	Skaugset and Baarholm [5]
Roughness coefficeint, *k/D*	0.28×10^{-3} – 1.38×10^{-2}	0.26×10^{-3} – 9.7×10^{-2}	0.26×10^{-3} – 0.197×10^{-3}	1.4×10^{-3} – 4.2×10^{-3}	12.0×10^{-3} – 0.114×10^{-3}	2.8×10^{-3} – 2.5×10^{-2}	5.88×10^{-2}	0.39 - 0.78
Roughness texture	Sand paper	Strips	Strips	Strips	Sand paper	Netting and dimple	Pyramidal pattern	Gravel

For sandpaper method, the roughness size of the surface texture was determined by its grit size and thickness of the support base [9]. The grit designation can be referred to determine the suitable sandpaper grades, corresponding average particles diameters, *k* and roughness coefficient, C_R for the experiment. If the dimple method is selected, one should consider the ratio, depth and spaces of the dimple. For example, Zhou *et al.,* [12] used 12 equally spaced dimples along the circumference, 0.05D of dimple radius 0.05D and the 0.009D of dimple depth, where D is the diameter of the cylinder. Result of Zhou *et al.,* [12] shows that the dimple cylinder reduces the recirculation region in the wake of the cylinder for the Reynolds number range 20,000 ≤ Re ≤ 80,000. If gravels are chosen, different materials should be used in modelling soft and hard marine growth. Skaugset and Baarholm [5] modelled hard marine growth such as barnacles on riser using can pebbles of various sizes while the soft marine growth such as marine grass was simulated using different types of fabrics, carpets or yarn with specific lengths and density. The growth rate of the marine fouling also affects the effectiveness of simulating the roughness texture. Skaugset and Baarholm [5] categorized the length of the soft marine fouling from 100 to 1000 mm and the height of the hard marine fouling from 10 to 50 mm. Zeinoddini *et al.,* [4] used pyramidal pattern to simulate the marine growth, which was early done by Wolfram in 1989. The selection is made due to the difficulties in VIV test.

Based on literature studies, it is learnt that there are a few methods that have been utilized in simulating the roughness around the body in both in-line and transverse directions. However, investigation on the effect of roughness towards VIV in purely transverse direction is somehow very

few. Hence, the objective of this paper is to investigate the amplitude response of the flexibly mounted pipe at different surface roughness through the utilization of different roughness of sandpapers. It is important to note that this study provides the basic or fundamental results of the different surface roughness effects towards VIV response. The framework of the present research is arranged as follows. In Section 2, the experimental setup and actuation system with its instrumentation are described. Then, the results of bare pipe, passive, and real-time active control implementation are presented in Section 3. The conclusion derived from the present study is presented in Section 4.

2. Experimental Setup

The experiments were conducted in a low-speed water channel tank at the Universiti Teknologi Malaysia's laboratory as shown in Figure 1. The water channel tank is 8 m long, 0.5 m channel-width and has a water depth of 0.5 m. The water channel tank is equipped with a large-volume displacement pump located at one end of the tank to generate circulating water flow inside the tank. The large-volume displacement pump controls the velocity of the water through the variable speed controller with maximum velocity of 0.4 m/s, measured at the model location. Based on the previous calibration, the velocity of the water fluctuates less 5 % at all speeds. More details can be found in [13].

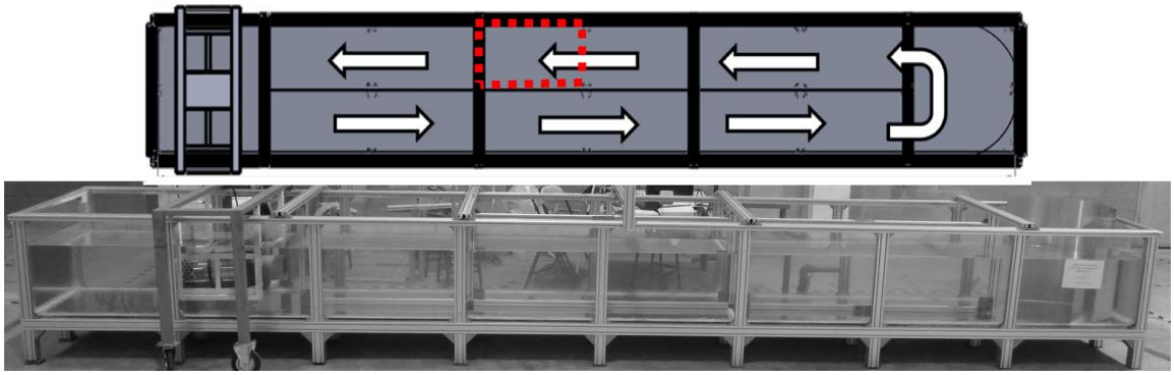

Fig. 1. The circulating water tank with effective working section region in dotted line [14]

The cylinder model used for this experiment is made of hollow aluminium pipe. This cylinder model has specific design characteristics, which are 615 mm in length and 51 mm of the outer diameter. A pair of end cap was secured at both ends of the cylinder model to prevent the water from entering into the pipe. This pipe will submerge into the water at length of 460 mm, and it has a small aspect ratio (L/D) of 12.06, which indicates that the model will not bend as water passes through the model. The detailed parameters of the cylinder model are listed in Table 2. Also, a pair of a circular acrylic plate with the dimension of 180 mm of outer diameter and 8 mm of the thickness was installed at the end of the cap to avoid three-dimensional flow effects and local ventilation of vortices. Then, this watertight cylinder model is attached to the linear slider at its both ends. This slider will ensure that the cylinder model to vibrate in transverse vibration and correspond to a single degree of freedom only. To ensure the pipe moving laterally four pieces of tension spring with a total of 140.0 N/m stiffness were connected to the circular acrylic plate, and this experimental setup is shown in Figure 2.

According to M. Zeinoddini [4] the standard size of the marine aquatic that grows on the surface of the marine structure is around 100 to 1000 mm length and 10 to 50 mm height. The data from

Table 1 were studied to get the appropriate roughness coefficient for this experiment. Since this experiment utilizes sandpaper in representing the surface roughness, hence, all the data that had been analyses will be transformed into sandpaper grit designation. From the data, there is certain roughness that still yet to be investigated. So, for this research, the scale of the roughness that was selected for the circular cylinder is P2000 to P60. Besides that, the surface roughness will be modelled by glueing the sandpaper on the surface of the circular cylinder. The sandpaper grades, corresponding average particle diameter, k and roughness coefficient, k/D are listed in Table 3.

Table 2
Physical properties of the vibrating body

Parameter	Symbol	Value	Units
Cylinder diameter	D	51	mm
Submerged length	L_S	460	mm
Aspect ratio	L/D	12.9	Dimensionless
Cylinder mass	m	1.32	Kg
Mass ratio	m^*	1.184	Dimensionless
System stiffness	K_S	140	N/m

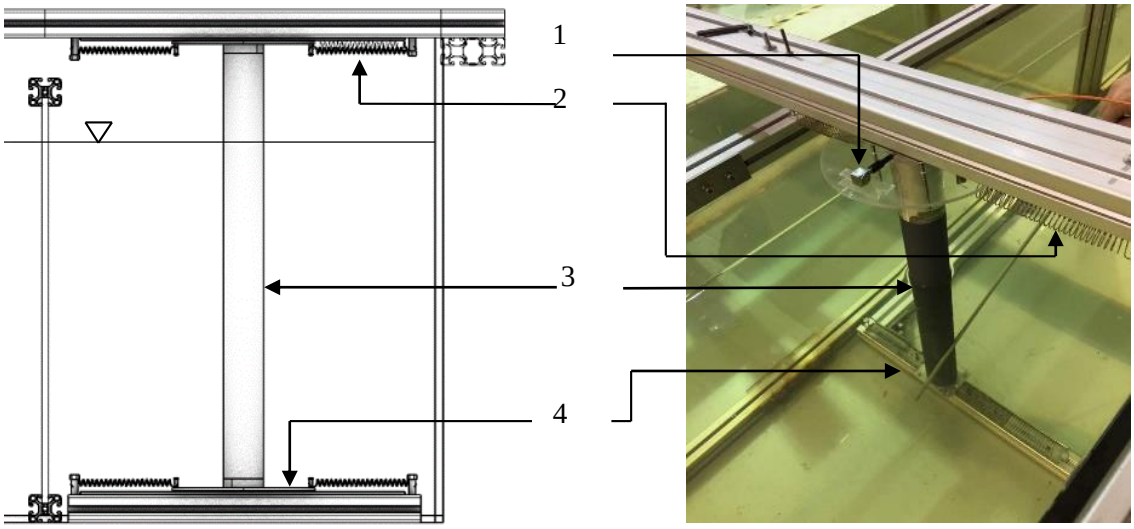

Fig. 2. Arrangement of elastically mounted circular cylinder in upright direction. Schematic 2D Model (left) and Actual photo (right) of the model in the Low Speed Water Tank. 1 – Accelerometer; 2 – Extension Spring unit; 3 – Submerged cylinder region; 4 – Splitter plate

Table 3
Grit designation with roughness coefficients

Grit designation	k (μm)	k/D
P 60	260	5.10×10^{-3}
P 320	46.2	0.91×10^{-3}
P 1000	18.3	0.36×10^{-3}
P 2000	9.6	0.19×10^{-3}

This experiment requires a personal computer (PC), Analog to Digital (A/D) converter and accelerometer for data collection purpose. A Dytran 3217A model of accelerometer was placed at the top of circular acrylic plate as shown in Figure 2 as labelled in 1. This accelerometer is used to measure the acceleration of the model as the model starts vibrating. The accelerometer will convert the acceleration data into an electrical signal for data collection process. Then, for personal computer to be able to read the data from the accelerometer, the electrical signal must be conditioned before

it can be converted from analogue signal to digital signal by using Digital (A/D) converter that has been installed into NI-PCI-62501 module. Finally, the data will be analyzed by using Dewesoft software. Integration from acceleration to displacement is made within the software. In most experimental works, noise such as white noise and electrical noise existed during the data collection process and it is unavoidable. The measured signal from the accelerometer cannot be used directly without pre-processing stage which the data is filtered where the noise or high-frequency signal is eliminated from the data. The filtered data is double integrated to obtain the displacement of the cylinder. Double integration can be done by using Matlab coding, which requires a set of coding with a specific constant. The other way around is by using Dewesoft where the acceleration of the cylinder can be integrated twice and the output can be obtained instantly during measurement in real-time. However, the only required parameter in utilizing embedded integration process in Dewesoft is the value of f_{low}, which is the lowest allowed frequency. In this experimental works, the value of f_{low} is set to be 1.61 Hz, which determined by the 1.5 times of the natural frequency of the system.

3. Results

3.1 Free Vibration Test

Free vibration test was performed to determine the natural frequency, f_n and damping parameter, ζ of the flexibly mounted cylinder system. It is done by measuring the cylinder displacement with respect to time after applying and releasing an initial transverse displacement to the main cylinder. Since the cylinder is restricted to move in transverse direction, only a single dominant frequency will exist. The natural frequency is determined by the Fast Fourier Transformation (FFT) and it was found that the natural frequency, f_n of the flexibly mounted system in still water is 1.074 Hz. Figure 3 shows the time history response of the still water decay test and the Fast Fourier Transformation (FFT) of the vibrating system. In relation with other dimensionless parameters, the value of f_n is utilized in calculating the reduced speed, U_r which is defined as in Eq. (1).

$$U_r = V/(f_n D) \tag{1}$$

where V is the measured velocity flow at the location of the modelled pipe and D is the external diameter of the cylinder. Meanwhile, the damping ratio can be obtained by using the log decrement method defined as in Eq. (2).

$$\zeta = \frac{\ln(Y_N/Y_{N+1})}{2\pi\delta} \tag{2}$$

where Y_N is the displacement amplitude of the N-th cycle, Y_{N+1} is that of the (N+1)-th cycle. From this equation, the structural damping parameter, ζ calculated for this system is 0.110. It is worth to note that besides the natural frequency, f_n, there are another three different frequencies that normally associated with VIV which are oscillating frequency f_o, vortex shedding frequency f_v and Strouhal frequency f_s. Oscillating frequency f_o is defined as the frequency of the measured displacement of cylinder for a specific period of time. Meanwhile, vortex shedding frequency can be defined as the rate of true vortices shed at certain period of time. Strouhal frequency is calculated as in Eq. (3).

$$f_{st} = St(\frac{V}{D}) \tag{3}$$

where St is the Strouhal number which usually defined as a constant.

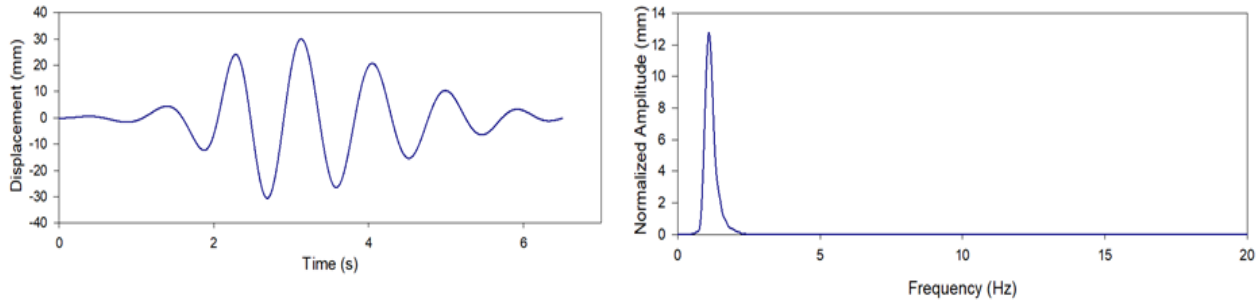

Fig. 3. Still water decay test time history (left) and FFT (right)

3.2 Cylinder Model Response: Bare Pipe

Before investigating the effect of surface roughness on the modelled pipe, it is important to study the amplitude response of the bare cylinder. The bare cylinder response at various reduced speeds, which ranged from 2.39 until 7.10 is represented by dotted markers with a solid line as shown in Figure 4. It is noted that the maximum reduced speed with the existing experimental setup is 7.10. At reduced speed ranged from 2.39 to 3.50, the system is believed to be within the initial excitation branch. Meanwhile, the upper branch is observed in reduced speed range of 3.87 and 7.04. Comparisons had been made with previous studies by Hover-Triantafyllou [15], Khalak-Williamson [16] and Brankovic-Bearman [17] for cylinder response at low mass ratio and plotted on the same Figure 4. It is important to note that the values of *A*/*D* obtained in this experiment are slightly lower and the reduced velocity range in upper branch is broader due to relatively high mass-damping ratio used in the experiment which is 0.130. However, the results obtained from the experimental work with mass ratio of 1.184 are in a good agreement with previous experimental results. The trend of increasing mass ratio is observed in the same Figure 4. It is noted that the uncertainty of experimental data is vital to ensure that the measurements have the lowest error as possible. The error of the amplitude ratio, A/D and reduced speed, U_r is estimated to be ± 0.03, and ± 0.05, respectively as the measurement chain includes the sensors and its signal conditioning.

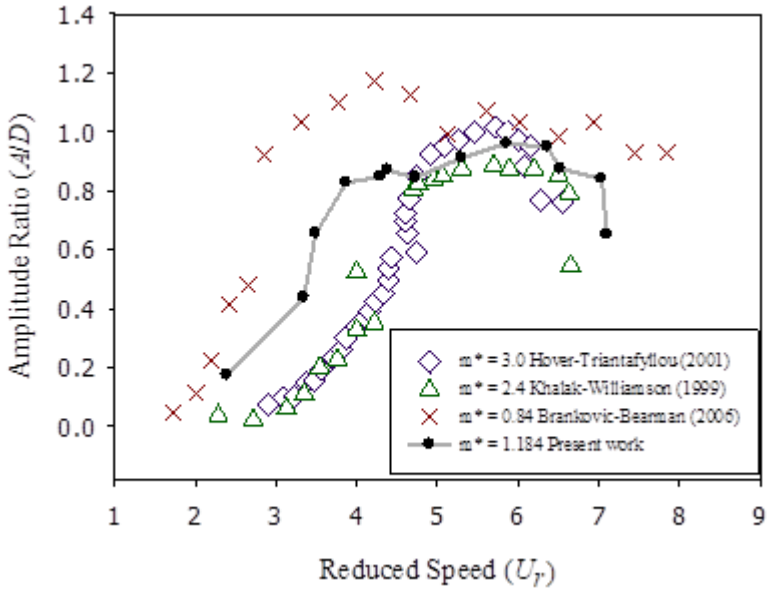

Fig. 4. Amplitude response of bare pipe for every reduced speed, U_r

3.3 Cylinder Model Response: Bare Pipe With Different Surface Roughness

The effect of surface roughness in pure transverse direction is then studied by covering the bare pipe with sandpaper of four different roughness coefficient. Figure 5 and 6 show the time history response of the modelled pipe with different roughness at single speed within initial and upper branches, respectively. It can be seen that the maximum amplitude is obtained by roughness coefficient $k/D = 0.19\times10^{-3}$, followed by 0.36×10^{-3}, 0.91×10^{-3} and 5.1×10^{-3}, respectively. Fast Fourier Transformation of the time history response was plotted and it was calculated that at initial branch region, the vibrating frequency increases as the roughness increases. The vibrating frequency of rough cylinder with roughness coefficient $k/D = 0.19\times10^{-3}$ is equal with the natural frequency of the smooth cylinder. However, due to its roughness, the amplitude is much lower as compared with a smooth cylinder. According to Kiu *et al.,* [7], the natural frequency of the roughest cylinder is about 4 percent lower than the smooth cylinder. Hence, it explains the reason for small amplitude at vibrating frequency of 1.074 Hz. Time history response for smooth cylinder can be seen in [13].

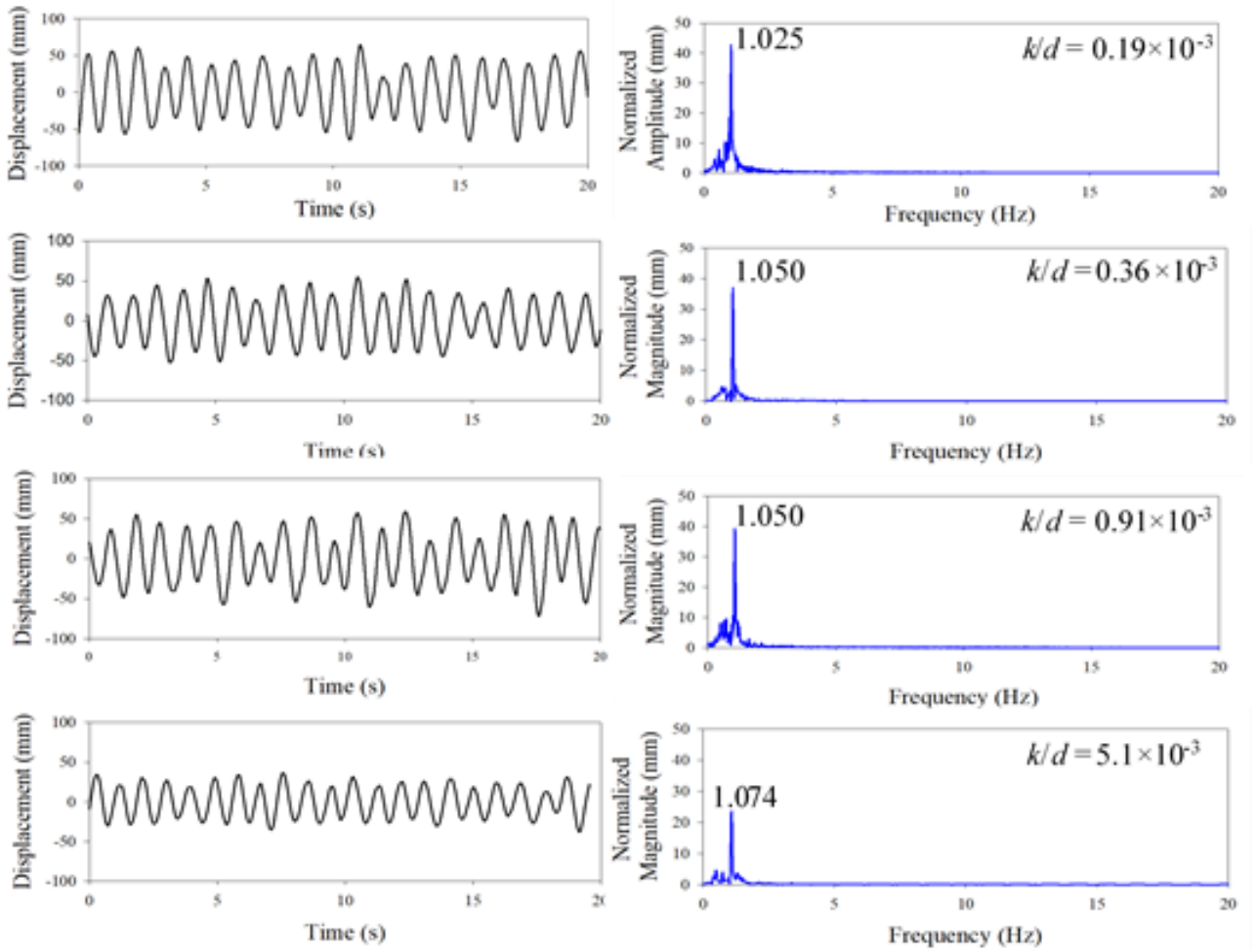

Fig. 5. Time history response of different roughness coefficient at $U_r = 3.6$

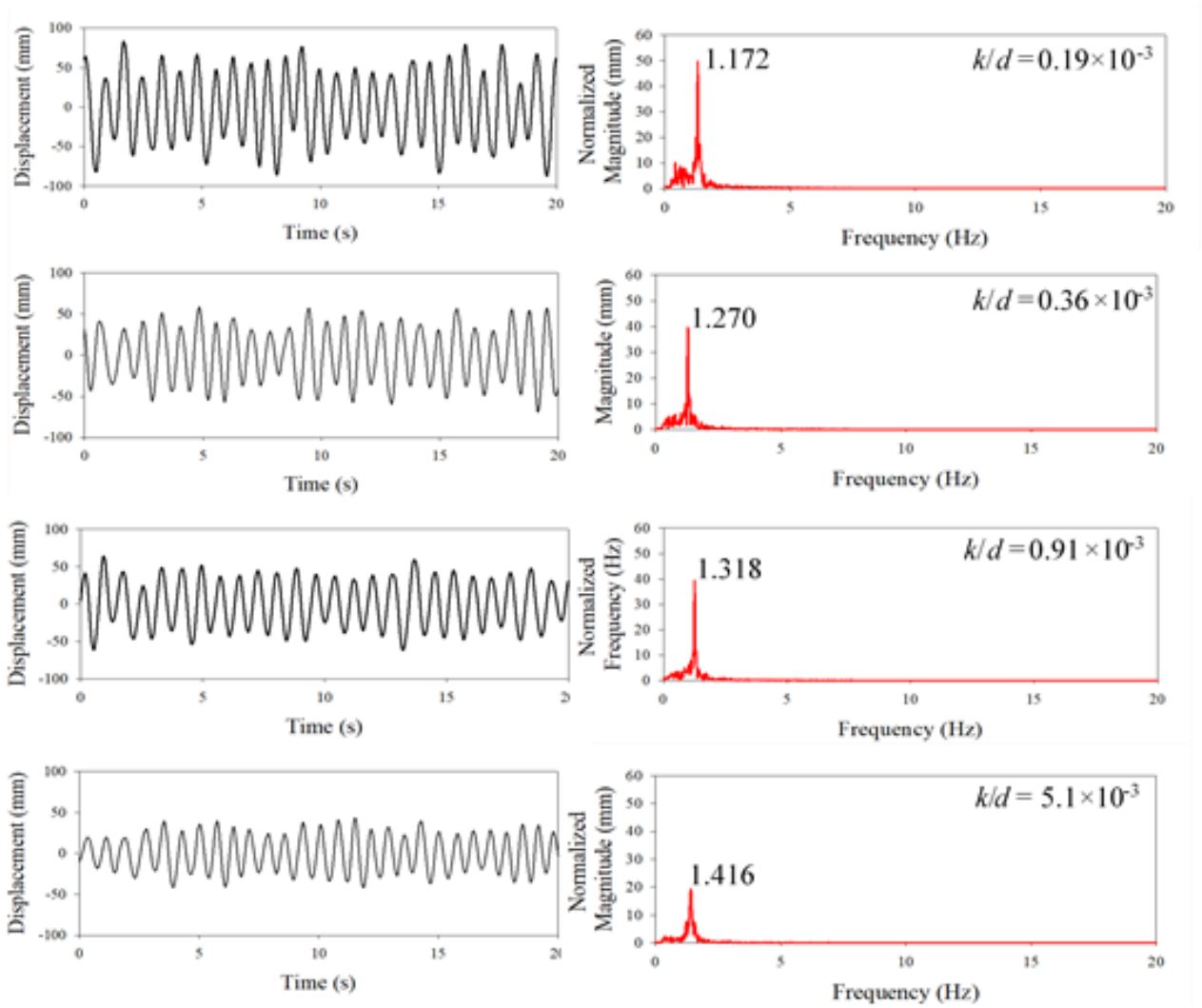

Fig. 6. Time history response of different roughness coefficient at U_r = 5.4

Meanwhile, the amplitude ratio response of a smooth and rough cylinder at different reduced speed are shown in Figure 7. The smooth cylinder response is represented by a solid circle with a solid connecting line, while the rest are rough cylinder response at different roughness coefficients. It is noted that two branches, which are the initial and upper branches are seen in the graph. It is perceived that as the surface roughness increases, the amplitude ratio decreases. Significant reduction of amplitude ratio is obtained by the roughest surface which the value of roughness coefficient is 5.1×10^{-3}. As reported by Kiu *et al.,* [7], the reduction in amplitude response is due to the delayed separation point. This happens because of the roughness surface introduces premature turbulences to the boundary layer. When the process of transition to turbulent modes happen, the boundary layer will increase the energy to the flow and this would lead to the formation of narrow wakes aft of the body. Figure 8 shows the result for the non-dimensional frequency of the smooth and rough cylinder at different roughness coefficient against varying reduced speed. The non-dimensional frequency is calculated by dividing the oscillating frequency, f_{osc} with the natural frequency of the system, f_n. Lock-in conditions were observed at certain reduced speeds, where the ratio between the oscillating and natural frequencies is equal to one.

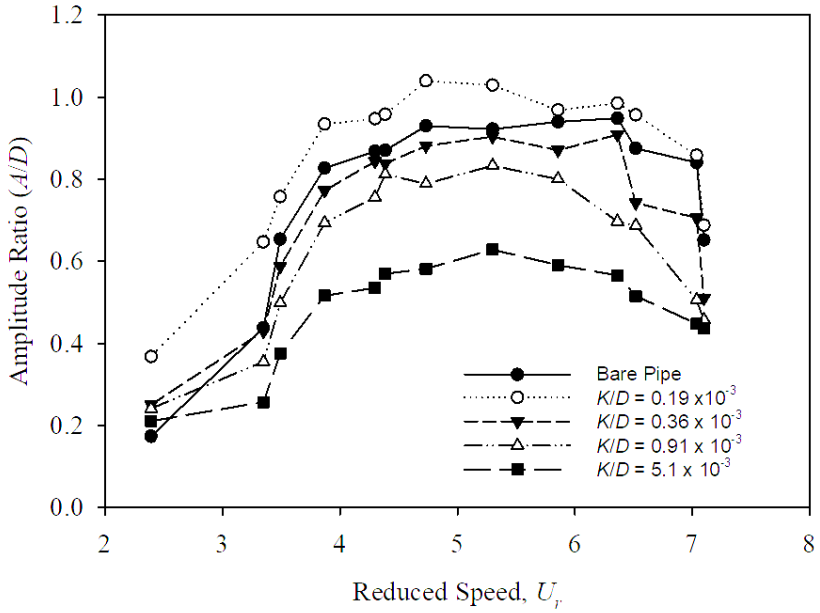

Fig. 7. Amplitude ratio of smooth and different roughness coefficient cylinder at varying reduced speed, U_r

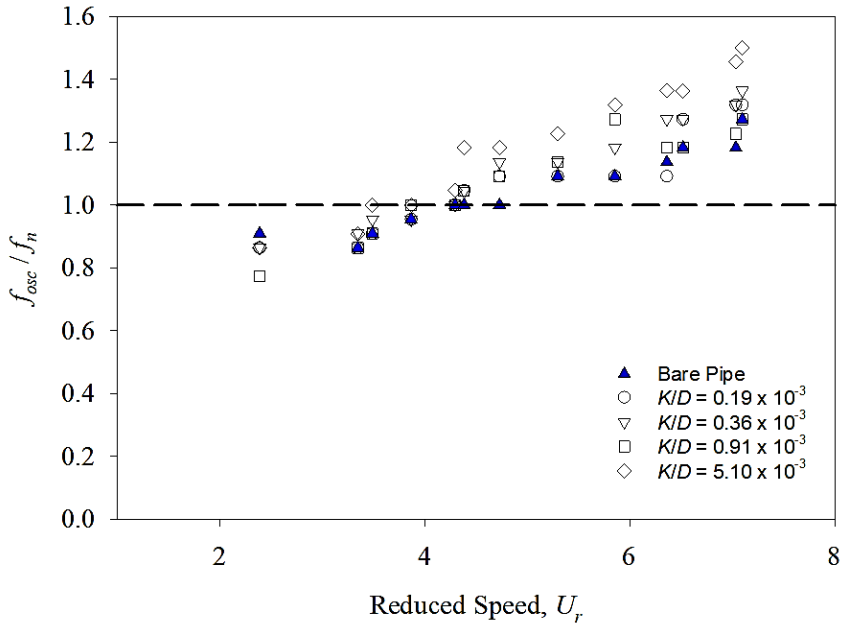

Fig. 8. Frequency ratio of smooth and different roughness coefficient cylinder at varying reduced speed, U_r

4. Conclusions

The investigations of roughness effect towards the vortex-induced vibration in pure transverse direction of a bluff body were presented in this paper through experimental works. The free vibration test was initially conducted to determine the system's natural frequency and damping coefficient. Then, the smooth cylinder response is then measured at different reduced speeds. In simulating different roughness on the cylinder body, four different roughness coefficients were utilized in the study. Based on the experiments, it was found that as the roughness increases, the amplitude response of the vibrating system decreases, which is due to the formation of narrow wake regions

behind the cylinder. For an instant, as much as 34.4 % of amplitude reduction has been obtained for roughness coefficient of 5.10×10^{-3} at reduced speed of 5.4. Besides that, as the roughness increases, the frequency of the vibration system was found to be increased even though the vibration amplitude is small.

Acknowledgement
This research was funded by Internal Research Grant Universiti Teknologi Malaysia (15H71) and grant from Ministry of Higher Education of Malaysia (FRGS Grant No: 5F129).

References

[1] Pastò, S. "Vortex-induced vibrations of a circular cylinder in laminar and turbulent flows." *Journal of Fluids and Structures* 24, no. 7 (2008): 977-993.
[2] Molland, Anthony F., ed. *The maritime engineering reference book: a guide to ship design, construction and operation*. Elsevier, 2011.
[3] Schoefs, Franck. "Sensitivity and Uncertainty Studies for the Modelling of Marine Growth Effect on Offshore Structures Loading." In *Proceedings of 21st International Conference on Offshore Mechanics and Arctic Engineering*, (2002): 1-7.
[4] Zeinoddini, M., A. Bakhtiari, M. Ehteshami, and M. S. Seif. "Towards an understanding of the marine fouling effects on VIV of circular cylinders: response of cylinders with regular pyramidal roughness." *Applied Ocean Research* 59 (2016): 378-394.
[5] Skaugset, Kjetil, and Rolf Baarholm. "Effect of marine growth on an elastically mounted circular cylinder." In *ASME 2008 27th International Conference on Offshore Mechanics and Arctic Engineering*, pp. 855-861. American Society of Mechanical Engineers Digital Collection, 2008.
[6] Gao, Yun, Shixiao Fu, Jungao Wang, Leijian Song, and Yifan Chen. "Experimental study of the effects of surface roughness on the vortex-induced vibration response of a flexible cylinder." *Ocean Engineering* 103 (2015): 40-54.
[7] Kiu, K. Y., Brad Stappenbelt, and K. P. Thiagarajan. "Effects of uniform surface roughness on vortex-induced vibration of towed vertical cylinders." *Journal of Sound and Vibration* 330, no. 20 (2011): 4753-4763.
[8] Zhou, Bo, Xikun Wang, Wie Min Gho, and Soon Keat Tan. "Force and flow characteristics of a circular cylinder with uniform surface roughness at subcritical Reynolds numbers." *Applied Ocean Research* 49 (2015): 20-26.
[9] Bernitsas, Michael M., Kamaldev Raghavan, and G. Duchene. "Induced separation and vorticity using roughness in VIV of circular cylinders at 8× 103< Re< 2.0× 105." In *ASME 2008 27th international conference on offshore mechanics and arctic engineering*, pp. 993-999. American Society of Mechanical Engineers Digital Collection, 2008.
[10] Chang, Che-Chun Jim, R. Ajith Kumar, and Michael M. Bernitsas. "VIV and galloping of single circular cylinder with surface roughness at 3.0× 104≤ Re≤ 1.2× 105." *Ocean Engineering* 38, no. 16 (2011): 1713-1732.
[11] Park, Hongrae, R. Ajith Kumar, and Michael M. Bernitsas. "Enhancement of flow-induced motion of rigid circular cylinder on springs by localized surface roughness at 3× 104≤ Re≤ 1.2× 105." *Ocean Engineering* 72 (2013): 403-415.
[12] Zhou, Bo, Xikun Wang, Wei Guo, Wie Min Gho, and Soon Keat Tan. "Experimental study on flow past a circular cylinder with rough surface." *Ocean Engineering* 109 (2015): 7-13.
[13] Shaharuddin, N. M. R., and IZ Mat Darus. "Experimental study of vortex-induced vibrations of flexibly mounted cylinder in circulating water tunnel." *Acta Mechanica* 226, no. 11 (2015): 3795-3806.
[14] Shaharuddin, Nik Mohd Ridzuan, and Intan Zaurah Mat Darus. "Implementation of active control on flexibly mounted pipe exposed to vortex induced vibration using rotating rod." *Meccanica* 53, no. 8 (2018): 2091-2103.
[15] Hover, F. S., H. Tvedt, and M. S. Triantafyllou. "Vortex-induced vibrations of a cylinder with tripping wires." *Journal of Fluid Mechanics* 448 (2001): 175-195.
[16] Khalak, A., and Charles HK Williamson. "Motions, forces and mode transitions in vortex-induced vibrations at low mass-damping." *Journal of fluids and Structures* 13, no. 7-8 (1999): 813-851.
[17] Branković, M., and P. W. Bearman. "Measurements of transverse forces on circular cylinders undergoing vortex-induced vibration." *Journal of fluids and structures* 22, no. 6-7 (2006): 829-836.